Oceanologia (2015) 57, 308—317

Available online at www.sciencedirect.com

ScienceDirect

journal homepage: www.elsevier.com/locate/oceano

OCEANOLOGIA

ORIGINAL RESEARCH ARTICLE

Numerical study of wave transmission over double submerged breakwaters using non-hydrostatic wave model☆

Bingchen Liang [a,b,*], **Guoxiang Wu** [a], **Fushun Liu** [a], **Hairong Fan** [a], **Huajun Li** [a]

[a] *College of Engineering, Ocean University of China, Qingdao, China*
[b] *Shandong Province Key Laboratory of Ocean Engineering, Ocean University of China, Qingdao, China*

Received 5 December 2014; accepted 9 July 2015
Available online 23 July 2015

KEYWORDS
Submerged breakwaters;
Wave transmission;
SWASH;
Numerical simulation;
Non-hydrostatic

Summary In the present work, a non-hydrostatic wave model SWASH (an acronym of Simulating WAves till SHore) is used to simulate the wave transmission over double trapezoidal submerged breakwaters. The numerical results were compared with the results of the physical model. The comparison indicated the capability of SWASH model to predict the wave transmission over double submerged breakwaters. Influencing factors such as breakwater spacing S/L_0, where L_0 is the deep-water wavelength, and current were investigated in detail. Moreover, the effects of current on wave transmission were also analyzed. When the relative submerged depth R/H, where R is the submerged depth and H is the wave height, remains at 1.0, the appropriate relative breakwater spacing S/L_0 is about 1.11. Current has no obvious effect on the appropriate S/L_0, but it will change the shape of wave spectrum. Dissipation of super harmonic wave components is more obvious than that of lower harmonic wave components.

☆ The authors would like to acknowledge the support of The National Science Fund (Grant No. 51179178), The Program for New Century Excellent Talents in University of China (Grant No. NCET-11-0471) and the 111 Project (B14028).
* Corresponding author at: Shandong Province Key Laboratory of Ocean Engineering, Ocean University of China, 238, Songling Road, Qingdao 266100, China. Tel.: +86 532 66781129; fax: +86 532 66781550.
E-mail address: bingchenliang@aliyun.com (B. Liang).
Peer review under the responsibility of Institute of Oceanology of the Polish Academy of Sciences.

Production and hosting by Elsevier

http://dx.doi.org/10.1016/j.oceano.2015.07.002

1. Introduction

It is a common practice to build submerged breakwaters in coastal areas to protect vessels, facilities, and coastal buildings against wave erosion. Because submerged breakwaters can attenuate waves, they are of great demand in coastal areas, especially in regions of scenic beauty. Hence, it is important to investigate the wave transformation processes and its dynamic characteristics around submerged breakwaters.

Recently, many scholars have conducted studies on wave propagation over submerged breakwaters. Beji and Battjes (1993) performed laboratory experiments to elucidate the phenomenon of high-frequency energy generation as waves propagate over submerged bars. They found that the bound harmonics were amplified during the shoaling process and released in the deeper water region after the breakwater crest. Based on a three-dimensional model, Andersen and Burcharth (2009) studied the influence of wave obliquity and directional spreading on waves overtopping of rubble mound breakwaters and proposed a method to estimate the overtopping discharge for head-on waves. Carevic et al. (2012, 2013) experimentally studied how the breakwater affects the changes of representative wave periods, when the waves propagate over the breakwater. Koraim et al. (2014) investigated the wave run-up on the seawall and the wave reflection in the presence of submerged breakwater, and studied the wave transmission over the submerged breakwater through physical experiments.

Many scholars have carried out analytical or numerical studies to predict the wave transmission across the breakwater. Sollitt and Cross (1972) derived a theory to predict ocean wave reflection and transmission at a permeable breakwater. The theory was found to match the experiment results. Ohyama and Nadaoka (1992) investigated a numerical model employing an effective non-reflective open boundary treatment based on the time-dependent boundary element method. They analyzed the super harmonics generated in the trailing side of the submerged breakwater. Van der Meer et al. (2000, 2003, 2005) developed a formula for predicting the transmission coefficient in a wide range of incident wave conditions and structure geometry. They also analyzed spectral changes and proposed in detail, a simple method for submerged breakwaters under breaking wave conditions. Briganti et al. (2003) studied the impact of the transmission coefficient on the transfer of energy from lower to higher harmonics and analyzed the evolution of wave spectrum shape preliminarily. Twu and Liu (2004) set up an analytical computational model to study the effects of porosity, number, width and height of bars on wave damping characteristics. They found that Bragg reflection generated by permeable bars is smaller than that generated by impermeable bars. Jeon and Cho (2006) investigated characteristics of the Bragg reflection due to multi-arrayed trapezoidal submerged breakwaters through numerical and experimental methods. The numerical model adopted in their study is based on the Reynolds averaged Navier—Stokes equations with the VOF method. According to their results, it is noted that the magnitude of velocity increases at the upper side of the first arrayed breakwater and decreases at the back side of the structures. In terms of their studies, the reflection coefficients increase as the array of submerged breakwaters increases. Wang et al. (2007) presented a series of analytical and numerical investigations in oblique wave transmission at low crested breakwaters. Their numerical simulations exhibited a significant decrease in the transmission coefficient with increase in oblique incidence attacking a smooth breakwater. Zou and Peng (2011) investigated the evolution of wave shape over a low crested structure using a 2D RANS VOF model. They found that wave skewness as a primary wave nonlinearity indicator varies across a submerged breakwater.

These studies mentioned above were on the hydrodynamic performance of single submerged breakwater without the existence of current. Possibly, both the number of submerged breakwater and current will affect the wave transmission. Therefore, Cao et al. (2012), based on N-S equation and VOF method, studied the hydrodynamic characteristics such as velocity field and turbulent kinetic energy in water waves propagating over two impermeable trapezoidal submerged breakwaters with 1:20 slope. They studied the wave attenuation rules of the submerged breakwaters with wave steepness. The effects of wave steepness have been discussed. He et al. (2007) adopted an analytic method to study the reflection and transmission coefficients of double submerged rectangle breakwaters in oblique waves and discussed the effects of geometric parameters and incident angle on the transmission and reflection coefficients in detail. They conclude that exchanging the positions of the two blocks does not affect the reflection and transmission coefficients for the fixed center distance. However, the current's effects on double submerged breakwaters have not been reported before. Moreover, numerical wave models built on the N-S equations with free surface tracking methods is time consuming. So it is very difficult to be a favorable choice to large-scale applications in coastal engineering.

The present work sets up several numerical models to simulate the wave propagation in a wave tank on the topography of double trapezoidal submerged breakwaters through SWASH model (an acronym of Simulating WAves till SHore). SWASH is a new time-domain wave propagation model based on the non-linear shallow water equations with non-hydrostatic pressure as referred in Zijlema et al. (2011). Suzuki et al. (2011) investigated the applicability of SWASH model for wave transformation and wave overtopping discharge by comparison with new physical model tests, indicating that SWASH model reproduces wave transformation and wave overtopping very well. Rijnsdorp et al. (2014) carried out numerical modeling of waves propagating over a plane slope and barred beach laboratory conditions through SWASH. The results when compared to the wave flume observations demonstrate that SWASH can be used to simulate the nearshore evolution of infragravity waves. The previous studies contribute wave transmission a lot. However, the present work focuses on studying the influences of relative breakwater spacing S/L_0, where L_0 is the deep-water wavelength, and current on wave propagation through numerical simulation, which will be useful references for submerged breakwater designing in the future. Accounting for the existence of narrow tide range in many seas, the present work fixed the relative submerged depth to a constant value of 1.0. Effects of variance of relative depth are not studied in the present work, which have been studied such as Cao et al. (2012) which has already proved that transmission coefficient rises with the increase in relative submerged water depth R/H, where R is the submerged depth and H is the wave height.

The present work is structured as follows. The theory of non-hydrostatic wave model SWASH is described in Section 2. Section 3 describes the validation of the numerical models with the data obtained from experiments carried out in The Ocean University of China. The results and discussions for wave transmission over double trapezoidal submerged breakwaters are given in Section 4. Finally, conclusions are drawn in Section 5 of the paper.

2. Theory description

SWASH is a numerical package developed by Delft University of Technology. It can simulate non-hydrostatic, free surface, and rotational flows in one and two horizontal dimensions (Zijlema et al., 2011). The governing equations are the nonlinear shallow water equations including a non-hydrostatic pressure term.

The equations are as follows:

$$\frac{\partial \zeta}{\partial t}+\frac{\partial hu}{\partial x}+\frac{\partial hv}{\partial y}=0, \tag{1}$$

$$\frac{\partial u}{\partial t}+u\frac{\partial u}{\partial x}+v\frac{\partial u}{\partial y}+g\frac{\partial \zeta}{\partial x}+\frac{1}{h}\int_{-d}^{\zeta}\frac{\partial q}{\partial x}dz+c_f\frac{u\sqrt{u^2+v^2}}{h}=\frac{1}{h}\left(\frac{\partial h\tau_{xx}}{\partial x}+\frac{\partial h\tau_{xy}}{\partial y}\right), \tag{2}$$

$$\frac{\partial v}{\partial t}+u\frac{\partial v}{\partial x}+v\frac{\partial v}{\partial y}+g\frac{\partial \zeta}{\partial y}+\frac{1}{h}\int_{-d}^{\zeta}\frac{\partial q}{\partial y}dz+c_f\frac{v\sqrt{u^2+v^2}}{h}=\frac{1}{h}\left(\frac{\partial h\tau_{yx}}{\partial x}+\frac{\partial h\tau_{yy}}{\partial y}\right), \tag{3}$$

$$w_b=-u\frac{\partial d}{\partial x}-v\frac{\partial d}{\partial y}, \tag{4}$$

$$\frac{\partial u}{\partial x}+\frac{\partial v}{\partial y}+\frac{w_s-w_b}{\partial t}=0. \tag{5}$$

Here, t is time, x and y the horizontal coordinates, $\zeta(x, y, t)$ the surface elevation from still water level, $d(x, y)$ the still water depth, $h = d + \zeta$ the total water depth, and $u(x, y, t)$ and $v(x, y, t)$ the depth-averaged flow velocity in x and y directions, respectively. $q(x, y, z, t)$ is the non-hydrostatic pressure at the bottom, g the gravitational acceleration, c_f the dimensionless bottom friction coefficient, τ_{xx}, τ_{xy}, τ_{yx} and τ_{yy} the horizontal turbulent stress terms, and w_b and w_s the vertical velocity at the bottom and at the free surface, respectively.

Moreover, SWASH adopts an explicit, second order finite difference method for staggered grids. The detailed descriptions of numerical implementation method are given in Zijlema and Stelling (2005) and Zijlema et al. (2011).

3. Numerical model

3.1. Model setting

The wave parameters were simulated using a non-hydrostatic wave prediction model, named SWASH. It modeled a vertical two-dimensional model using a horizontal grid size of 0.05 m and 10 layers in vertical direction with a time step of 0.02 s. Absorbing-generating boundary conditions are adopted at side of wave generator. Time series of water level generated by regular or irregular waves by means of a spectrum are inputted. A thick sponge layer was installed at the right boundary to avoid wave reflection, which is two to three times the wavelength. Water depth was divided into 10 layers vertically. Numerical model validation is described in Section 3.2. In order to study the effects of breakwater spacing S/L_0 and current on wave transmission, more numerical models were set up. The details of these models' settings are given in the following sections.

3.2. Model validation

To validate the SWASH numerical model, wave data from the physical experiments conducted in the laboratory of Ocean University of China were utilized. The wave tank was 60.0 m long and 3.0 m wide. A wave generator was used for wave generation in one end of the wave tank. Flows with $U = 0.1$ m s^{-1}, denoting the waves propagating with the tidal current, and $U = -0.1$ m s^{-1}, denoting the waves propagating against the tidal current, were generated, respectively. A sponge layer was deployed at the end of the wave tank to decrease wave reflection. The sponge layer consists of porous material made of iron wire. The thickness of the sponge layer is about 5 m. The submerged breakwater was 0.6 m high and the breakwater crest width was 2.9 m. The wave generator and the breakwater were located at $x = 0.0$ m and $x = 23.6$ m, respectively, as shown in Fig. 1. Four wave gauges (#1—#4) are placed along the wave tank for measuring free surface elevation. The wave gauges were positioned one each at the front, the slope, and the crown of the submerged breakwater, respectively and one after the submerged breakwater.

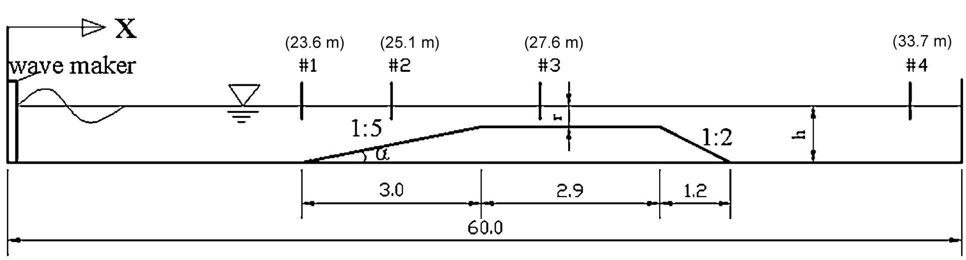

Figure 1 Experimental setup of wave transformation over submerged breakwater.

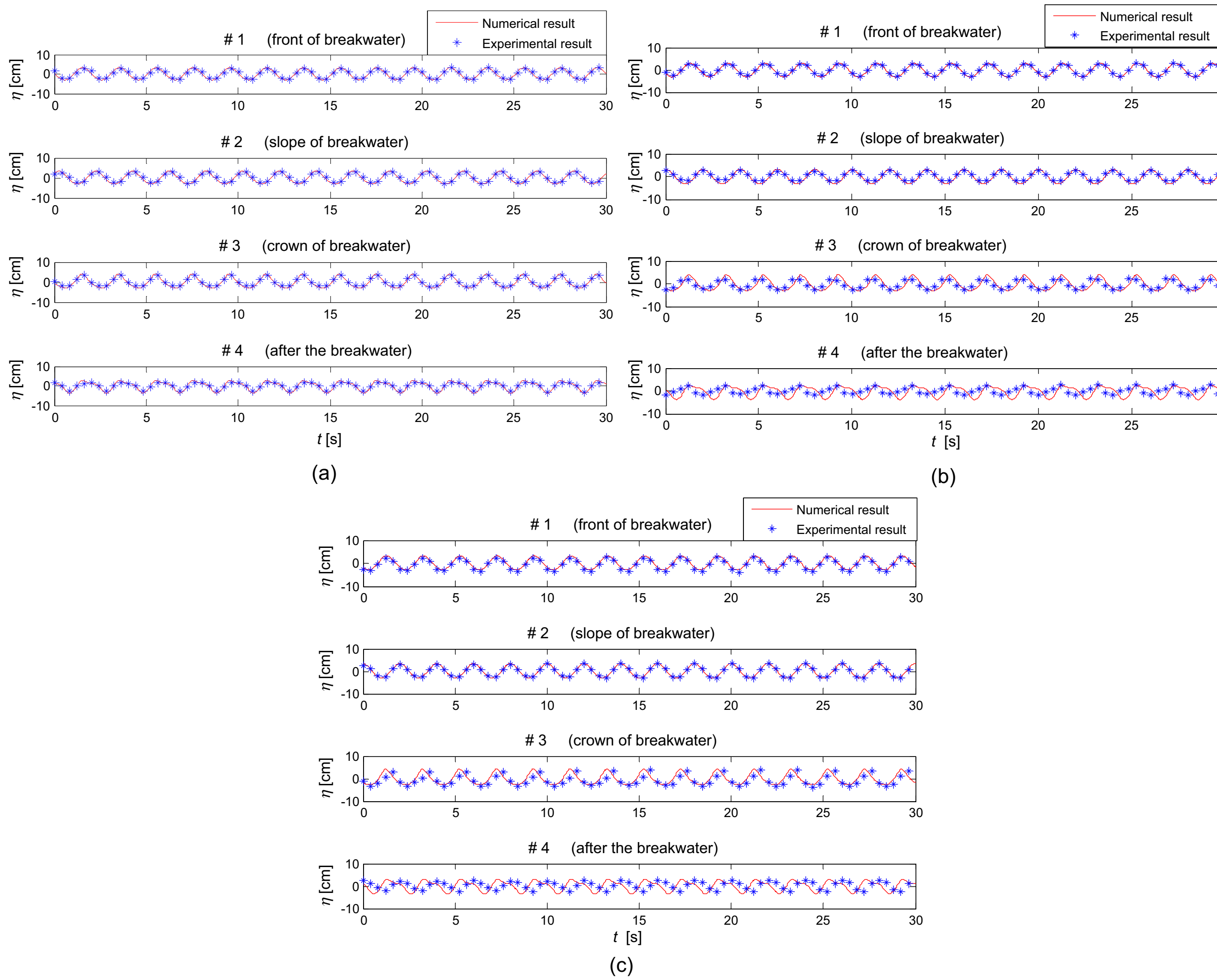

Figure 2 Validation for regular wave ($H = 0.05$ m, $T = 2.0$ s). (a) $U = 0$ m s^{-1}; (b) $U = 0.1$ m s^{-1}; (c) $U = -0.1$ m s^{-1}.

Each gauge obtains free surface elevation for 120.0 s with a sampling frequency of 50.0 Hz. The measurements were taken at the crown of the submerged breakwater, where the submersion is 0.35 m.

Fig. 2 shows the surface elevation comparison between the measured data and simulated results for regular waves. The incident wave height is 0.05 m and the wave period is 2.0 s. As we can see from Fig. 2, numerical results of the wave profiles correspond to the measured data for both pure wave and current wave conditions. In general, the validation indicates the capability of the SWASH model to predict accurately the regular wave transformation around submerged breakwaters. Correlation coefficient between results measured and results simulated is shown in Table 1, which indicates the capability of the SWASH model to predict accurately the regular wave transformation around submerged breakwaters generally. Shown in Fig. 2b and c, which give comparing curves, little phase lag is found at #4. During experiment processes, the current velocity is measured at #1 only. However, current velocity is not uniform along the whole tank. Specially, current velocity rises rapidly due to shallow effects of submerged breakwater. Around submerged breakwater, faster current may bring stronger interaction between current and wave. So wave and wave energy propagation velocity varies along the whole tank. Moreover, accounting for changes of turbulence energy and eddy viscosity induced by the interaction, wave transmission will also be changed furtherly due to the existence of uniform current. Therefore, some phase occurs at the location #4 being far away from #1 when current exist. Fig. 3 shows wave-surface elevation comparison between the measured data and the simulated data for irregular waves. The incident significant wave height is 0.05 m and wave period is 2.0 s. As we can see from this figure, the numerical results correspond with the experimental results, indicating that the non-hydrostatic wave model SWASH can also accurately simulate irregular

Table 1 Correlation coefficient.

Station	$U = 0$ m s^{-1}	$U = 0.1$ m s^{-1}	$U = -0.1$ m s^{-1}
#1	0.9838	0.9608	0.9697
#2	0.9720	0.9785	0.9607
#3	0.9305	0.8146	0.9785
#4	0.9040	0.7017	0.7971

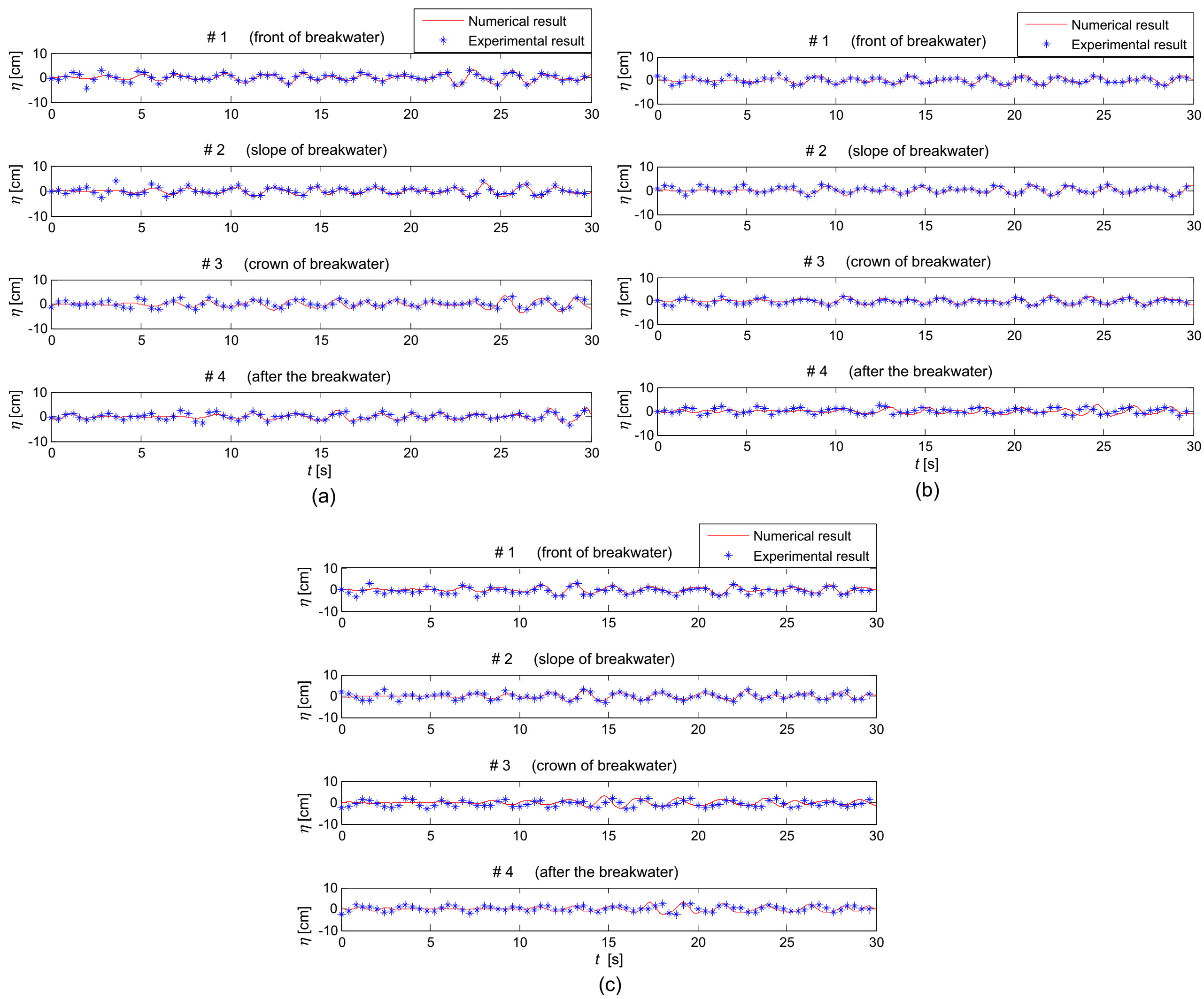

Figure 3 Validation for irregular wave ($H_{1/3}$ = 0.05 m, $T_{1/3}$ = 2.0 s). (a) U = 0 m s^{-1}; (b) U = 0.1 m s^{-1}; (c) U = −0.1 m s^{-1}.

wave propagation over the topography of submerged breakwater in the wave tank. Hence, the present model may be reliable to analyze the wave transformation over double trapezoidal submerged breakwaters.

4. Results and discussions

In order to investigate the influences of relative breakwater spacing S/L_0 on wave transmission, several numerical models on double submerged breakwaters were set up. The topography of double submerged breakwaters is shown in Fig. 4. The height of the two submerged breakwaters, width of the breakwater crest, water depth, and slope are 0.8 m, 1.0 m, 0.95 m, and 1:2, respectively. Tide range is relatively narrow in some areas of the sea, such as the western areas of Japan Sea. As a result, on setting up the numerical models, the present work investigated the effect of submerged breakwater spacing and current on wave transformation keeping the relative submerged depth as a constant with 1.0 value. The Cartesian coordinate system was established by defining the beginning of the wave tank as the origin, where the wave generator is placed. The first submerged breakwater was placed in 100 m long wave tank at the position x = 20.0 m. S represents the breakwater spacing, which is the distance between the two submerged breakwaters' center. The water depth on the submerged breakwater crown is represented as R.

The following section investigates the effect of relative breakwater spacing S/L_0 on wave propagation based on numerical simulations. It aims to find the most appropriate breakwater spacing S/L_0 as references for the practical engineering.

4.1. Effect of relative breakwater spacing S/L_0

Breakwater spacing has effects on the transmission coefficients and transmitted wave spectrum. In order to investigate the relationship between wave transmission and relative breakwater spacing, several numerical models with different topographies were set up. First, this section studies the breakwater spacing's effects on regular wave, when the incident wave height, period and water depth are 0.15 m, 2.0 s, and 0.95 m, respectively. The breakwater spacing S/L_0 varies from 0.67 to 1.31.

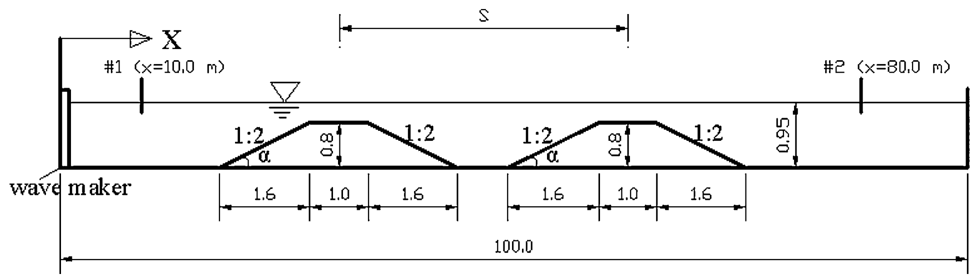

Figure 4 Details of the topography for numerical experiment.

Two-point method of Goda and Suzuki (1976) was employed to separate the incident and reflected waves. So incident wave height (H_i), reflected wave height (H_r), and transmitted wave height (H_t), can be obtained separately. Therefore, the transmission coefficient (K_t) and reflection coefficient (K_r), respectively, can be defined as follows:

$$K_t = \frac{H_t}{H_i}, \tag{6}$$

$$K_r = \frac{H_r}{H_i}. \tag{7}$$

Attenuation coefficient, K_a, can be obtained through the principle of energy conservation, and is defined as follows:

$$K_a = \sqrt{1 - K_t^2 - K_r^2}. \tag{8}$$

Fig. 5 shows the curves of transmission coefficient (K_t), reflection coefficient (K_r), and attenuation coefficient (K_a) against relative breakwater spacing S/L_0, for regular waves.

From Fig. 5, it is obvious that relative breakwater spacing affects the transmission and attenuation coefficients. The reflection coefficient changes from 0.35 to 0.4, which shows that the effects of relative breakwater spacing S/L_0 on reflection are not very obvious with constant relative submerged depth. The reflection in front of first submerged breakwater is more affected by the first submerged breakwater than the second one. The reflective waves from second submerged breakwater and super harmonic wave component are dissipated much when propagate cross the two arrays. The relative breakwater spacing S/L_0 can affect wave energy dissipation and transmission through increasing energy dissipation caused by strong current and wave interaction under complex topography. With the increase in relative breakwater spacing, K_t decreases initially and reaches a minimum value of 0.71, when S/L_0 is 1.11. Afterwards, when S/L_0 rises continuously K_t increases gradually. However, K_a shows the opposite tendency with the increase in relative breakwater spacing. The maximum value of K_a is close to 0.60 when S/L_0 is 1.11. In other words, the double submerged breakwaters showed better performance in reducing wave effects when the relative breakwater spacing was 1.11. When S/L_0 is 1.11, to investigate the wave energy dissipation during propagating submerged breakwaters, Fig. 6 shows the turbulent kinetic energy. It is easy to know that there are much turbulent kinetic energy around first array top of submerged breakwater. Moreover, obvious turbulence also appears around top of second breakwater. So more wave energy is dissipated to turbulence for two arrays of breakwater than single array.

On considering irregular waves, the target wave spectrum is JONSWAP spectrum. The incident significant wave height is 0.15 m and the significant wave period is 2.0 s. Here, the significant wave period means the averaged wave period of the largest 1/3 individual wave periods with descending list. The other parameters are same as those in the case of regular waves. Fig. 7 shows the transmission coefficients of irregular waves. The variation in K_t with relative breakwater spacing S/L_0 is similar to that of regular waves (shown in Fig. 5). When S/L_0 is 1.11, K_t becomes lowest being 0.421.

For irregular waves, Fig. 8 shows the wave spectrums behind the submerged breakwater for different breakwater

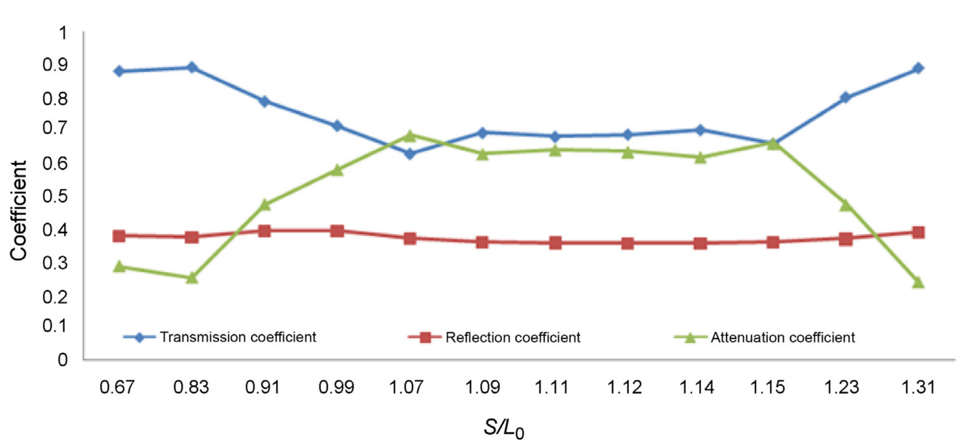

Figure 5 Variation in transmission coefficient K_t versus S/L_0 for regular waves.

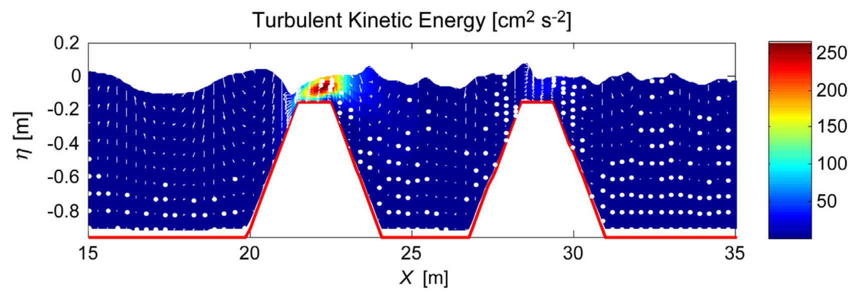

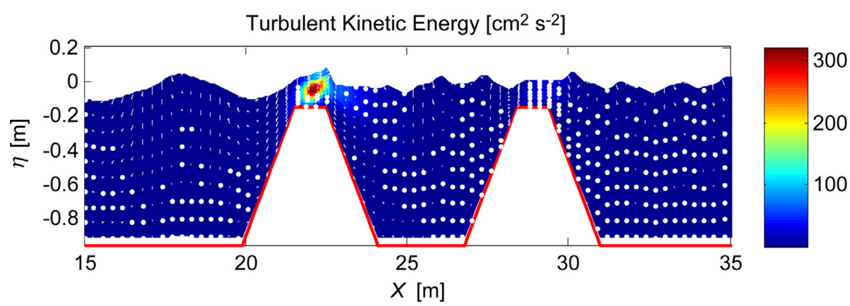

Figure 6 Turbulent kinetic energy distribution under regular wave (quivers stand for velocity vector). (a) Wave trough and (b) wave crest above first array submerged breakwater.

spacing conditions. It shows that the wave spectrums have similar shapes in both lower frequency and higher frequency domains. With the breakwater spacing increasing, more wave energy is shifted to the higher frequency domain, and the wave energy within the basic frequency domain decreases. From the figure, it is understood that the transmitted wave energy is lowest when relative breakwater spacing S/L_0 lies between 0.99 and 1.15.

To quantitatively investigate the wave's internal energy variation, the wave energy distribution of the transmitted wave for irregular wave is used, and is given in Table 2. E_i is the wave energy of the incident wave, E_t is the wave energy of the transmitted wave, and $E_{t1.5}$ is the transmitted wave energy within the high frequency domain, meaning wave energy in the range between 1.5 and 3.5 of peak frequency.

When waves pass over double submerged breakwaters, there are some internal changes in wave energy distribution. Some part of the energy is attenuated and some shift from the lower frequency domain to the higher frequency domain. In the present work, as mentioned in the above paragraphs, wave energy between 1.5 and 3.5 of peak frequency is defined as super harmonic wave, expressed by $E_{t1.5}$. Table 3 proves that super harmonic wave energy occupies 13.70—23.62% of the transmitted wave. The ratio $E_{t1.5}/E_t$ changes with the variation in breakwater spacing and tends to be minimum at 13.7%, when relative breakwater spacing is about 0.91. A portion of the wave energy is dissipated, whereas some portion is reflected by the submerged breakwater. Hence, the transmitted wave energy is about 20% of the incident wave energy. The ratio of transmitted wave

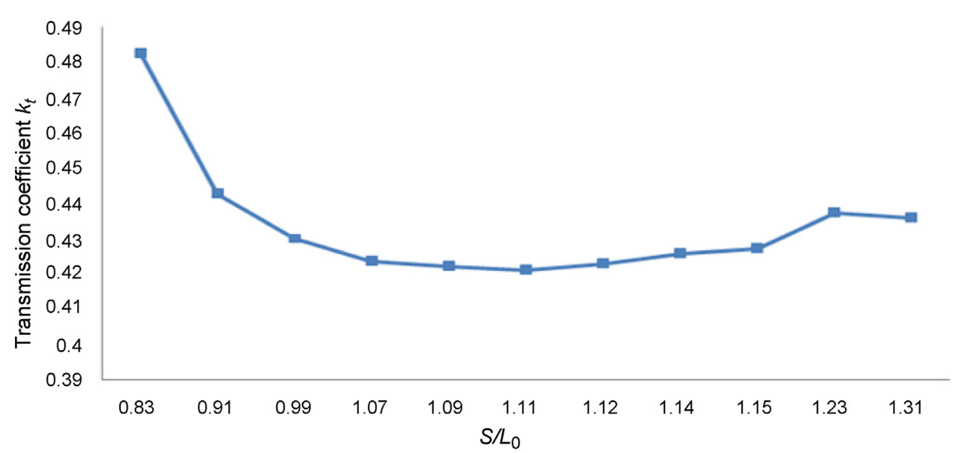

Figure 7 Variation in transmission coefficient K_t versus S/L_0 for irregular wave.

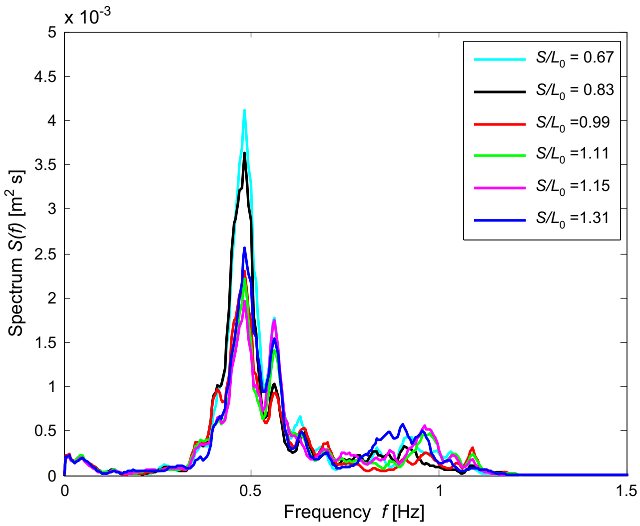

Figure 8 Transmitted wave spectrums for different breakwater spacing.

energy to incident wave energy decreases initially and then increases with the increase in relative breakwater spacing S/L_0.

Van der Meer et al. (2000) put forward constant distribution of wave energy on higher harmonics (40%); this is a very crude description of spectral distribution and inadequate to assume constant distribution of the wave energy on higher harmonics. Carevic et al. (2013) modified the empirical modeling of Van der Meer et al. (2000), proposed a linear formula of $E_{t1.5}/E_t$ to R_c/H and wave steepness s_{op}, as follows:

$$\frac{E_{t1.5}}{E_t} = \max[0.071, (-2.71s_{op} + 0.32)\frac{R_c}{H} + (-6.21s_{op} + 0.71)]. \tag{9}$$

Based on Eq. (6) for single submerged breakwater, $E_{t1.5}/E_t$ equals to 29.16% with R_c/H and wave steepness being same as those of the present study. In the present work, focusing on double trapezoidal submerged breakwaters, the wave energy of higher harmonics components changes from 13.7% to 23.62%. Based on Table 3, it is easy to find that wave energy of super harmonic components occupies 38.35% when wave transmits to middle of the two submerged breakwaters. However, at the same time, wave energy of super harmonic components decreases from 38.35% to 21.36% when waves propagate across second submerged breakwater, proving that dissipation of super harmonic wave components is more obvious than that of lower harmonic wave components. The differences between the present study and results given by Eq. (6) can be accepted when accounting for different slopes, single and double arrays of breakwaters etc. between the present studies and studies of Carevic et al. (2013).

4.2. Effect of current on appropriate breakwater spacing S/L_0

When relative breakwater spacing is around 1.11 with the relative submerged depth maintaining a constant of 1.0, the transmission coefficient is the smallest, confirming the capability of submerged breakwaters in reducing the wave energy. In the following paragraphs, the effect of current on appropriate breakwater spacing S/L_0 is investigated.

Fig. 9 shows the variation in transmission coefficients against the breakwater spacing changes for varying current

Table 2 Wave energy distribution of transmitted wave.

Test	E_t [$\times 10^{-3}$ m^2 s]	$E_{t1.5}$ [$\times 10^{-3}$ m^2 s]	$E_{t1.5}/E_i$ [%]	$E_{t1.5}/E_t$ [%]	E_t/E_i [%]
S/L_0 = 0.67	0.5478	0.0826	3.94	15.08	26.14
S/L_0 = 0.83	0.4712	0.0663	3.16	14.07	22.49
S/L_0 = 0.91	0.4123	0.0565	2.70	13.70	19.68
S/L_0 = 0.99	0.3801	0.0552	2.63	14.52	18.14
S/L_0 = 1.07	0.382	0.0733	3.50	19.19	18.23
S/L_0 = 1.09	0.3845	0.0789	3.77	20.52	18.35
S/L_0 = 1.11	0.3924	0.0838	4.00	21.36	18.73
S/L_0 = 1.12	0.3965	0.0883	4.21	22.27	18.92
S/L_0 = 1.14	0.4065	0.0923	4.41	22.71	19.40
S/L_0 = 1.15	0.4018	0.0949	4.53	23.62	19.18
S/L_0 = 1.23	0.4291	0.1012	4.83	23.58	20.48
S/L_0 = 1.31	0.4405	0.1030	4.92	23.38	21.02

Table 3 Comparison of wave energy distribution of transmitted wave for irregular wave.

Location	E_t [$\times 10^{-3}$ m^2 s]	$E_{t1.5}$ [$\times 10^{-3}$ m^2 s]	$E_{t1.5}/E_t$ [%]	E_t/E_i [%]	$(E_i - E_t)/E_i$ [%]
Between breakwaters	0.8896	0.3412	38.35	42.46	57.54
After breakwaters	0.3924	0.0838	21.36	18.73	81.27

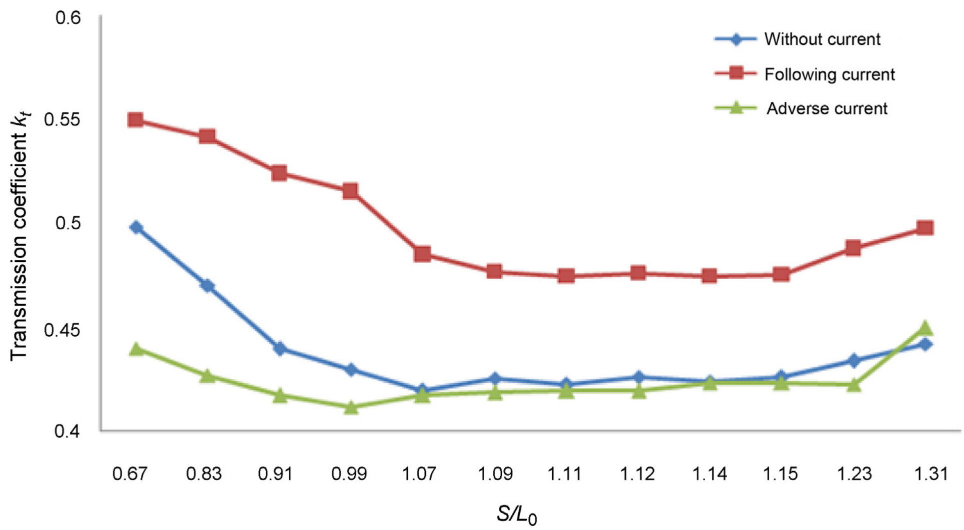

Figure 9 Variation in transmission coefficient K_t versus S/L_0 in different current conditions.

conditions. Essentially, transmission coefficient K_t changes with breakwater spacing and current. For all the three current conditions, following current, adverse current and no current, K_t exhibits the same variation tendency. It decreases initially and then increases with the rise in relative breakwater space. K_t tends to be the lowest when relative breakwater spacing ranges from 1.07 to 1.15. However, transmission coefficient has the largest value for following current condition and the lowest value for adverse current condition. This phenomenon indicates that the double trapezoidal submerged breakwater reduces wave energy better in adverse current conditions. In other words, submerged breakwaters influence the wave transformation more in ebb tide than in flood tide. Based on the above descriptions, it is obvious that K_t decreases initially and then increases with the rise in relative breakwater spacing irrespective of the current condition.

Fig. 10 shows the wave spectrums of irregular waves for different current conditions. It shows that the transmitted wave energy is the lowest in adverse current, which is similar to transmission coefficient shown in Fig. 9. In adverse current, a large portion of the wave energy is dissipated through wave breaking. For following current, in terms of Fig. 10, the wave height increases. Transmitted wave energy in the following current is larger than the other cases owing to lesser dissipation along the wave tank. In order to understand quantitatively, the wave energy distribution along the frequency domain, Table 4 is introduced to show the wave energy distribution of transmitted wave under different current conditions. The relative breakwater spacing, S/L_0 of all the cases is 1.11.

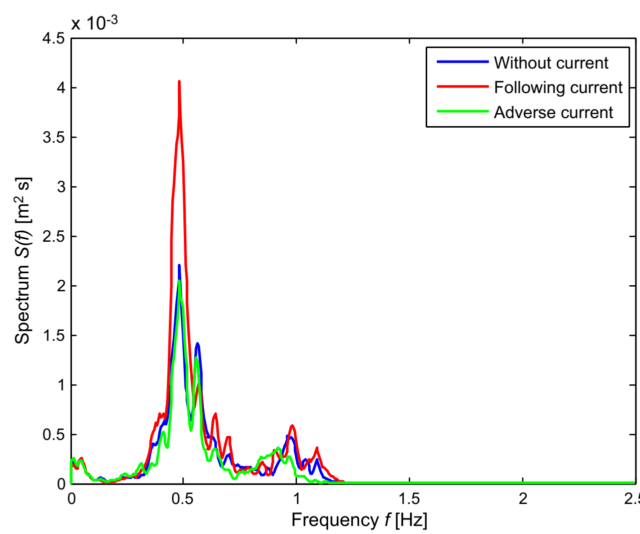

Figure 10 Wave spectrums of transmitted wave in different current conditions.

As shown in Table 4, wave energy after the submerged breakwater contains 15.66% of the incident wave energy in adverse current, which is low compared to following current and no current condition. In adverse current condition, more wave energy is dissipated and reflected by the submerged breakwater. In following current condition, more wave energy is transmitted from the lower frequency domain to higher frequency domain, compared to adverse and no current condition.

Table 4 Wave energy distribution of transmitted wave.

Test	E_t [$\times 10^{-3}$ m^2 s]	$E_{t1.5}$ [$\times 10^{-3}$ m^2 s]	$E_{t1.5}/E_i$ [%]	$E_{t1.5}/E_t$ [%]	E_t/E_i [%]
Without current	0.3924	0.0838	4.00	21.36	18.73
Following current	0.5511	0.0987	4.71	17.91	26.30
Adverse current	0.3282	0.0625	2.98	19.04	15.66

5. Conclusions

In the present work, SWASH is used to study the wave transmission as it passes over double submerged breakwaters. The following summaries are drawn:

First, the numerical model was validated for regular and irregular waves through surface profile and wave spectrum, respectively. The validation included cases irrespective of the existence of current. The validation indicates the capability of SWASH to simulate wave transformation over double submerged breakwaters under laboratory conditions.

Second, the influences of relative breakwater spacing and current on wave transformation along the wave tank were studied. It confirmed that the value of appropriate relative breakwater spacing S/L_0 was around 1.11, provided the relative submerged depth R/H is fixed to 1.0.

Third, dissipation of super harmonic wave components is more obvious than that of lower harmonic wave components.

Finally, regardless of following current or adverse current condition, the value of appropriate S/L_0 remains constant, however, the nonlinear effects between current and wave will change the wave spectrum.

Acknowledgements

The authors appreciate the reviewers for their suggestions and comments, which are very helpful to improve the manuscript.

References

Andersen, T.L., Burcharth, H.F., 2009. Three-dimensional investigations of wave overtopping on rubble mound structures. Coastal Eng. 56 (2), 180—189.

Beji, S., Battjes, J.A., 1993. Experimental investigation of wave propagation over a bar. Coastal Eng. 19 (1), 151—162.

Briganti, R., Van der Meer, J.W., Buccino, M., Calabrese, M., 2003. Wave transmission behind low crested structures. In: Proc. 3rd Coastal Structures Conference. 580—592.

Cao, Y., Jiang, C., Bai, Y., 2012. Wave attenuation properties of double trapezoidal submerged breakwaters on flat-bed. Trans. Tianjin Univ. 18, 401—410.

Carevic, D., Loncar, G., Prsic, M., 2012. Transformation of statistical and spectral wave periods crossing a smooth low-crested structure. Oceanologia 54 (1), 39—58.

Carevic, D., Loncar, G., Prsic, M., 2013. Wave parameters after smooth submerged breakwater. Coastal Eng. 79, 32—41.

Goda, Y., Suzuki, Y., 1976. Estimation of incident and reflected wave in random wave experiments. In: Proceedings of 15th Conference on Coastal Engineering, Honolulu, Hawaii, USA, 828—845.

He, Z., Liu, P., You, Y., Feng, B., 2007. Reflection and transmission properties of double submerged rectangular blocks. Acta Oceanol. Sin. 26 (2), 115—122.

Jeon, C.-H., Cho, Y.-S., 2006. Bragg reflection of sinusoidal waves due to trapezoidal submerged breakwaters. Ocean Eng. 33, 2067—2082.

Koraim, A.S., Heikal, E.M., Abo Zaid, A.A., 2014. Hydrodynamic characteristics of porous seawall protected by submerged breakwater. Appl. Ocean Res. 46, 114.

Ohyama, T., Nadaoka, K., 1992. Modeling the transformation of nonlinear waves passing over a submerged dike. Proc. Coastal Eng. 1 (23), 526—539.

Rijnsdorp, D.P., Smit, P.B., Zijlema, M., 2014. Non-hydrostatic modelling of infragravity waves under laboratory conditions. Coastal Eng. 85, 30—42.

Sollitt, C.K., Cross, R.H., 1972. Wave transmission through permeable breakwaters. Coastal Eng. Proc. 1 (13), 1827—1846.

Suzuki, T., Verwaest, T., Hassan, W., Veale, W., Reyns, J., Trouw, K., Zijlema, M., 2011. The applicability of SWASH model for wave transformation and wave overtopping: a case study for the Flemish coast. In: Proc. 5th Int. Conf. Advanced Computational Methods Engineering (ACOMEN 2011), Liège, Belgium, 14—17.

Twu, S.-W., Liu, C.-C., 2004. Interaction of non-breaking regular waves with a periodic array of artificial porous bars. Coastal Eng. 51, 223—236.

Van der Meer, J.W., Briganti, R., Zanuttigh, B., Wang, B., 2005. Wave transmission and reflection at low crested structures: design formulae, oblique wave attack and spectral change. Coastal Eng. 52 (10—11), 915—929.

Van der Meer, J.W., Regeling, H.J., de Waal, J.P., 2000. Wave transmission: spectral changes and its effects on run up and overtopping. In: Proc. 27th Int. Conf. Coast. Eng. ASCE. 2156—2168.

Van der Meer, J.W., Wang, B., Wolters, A., Zanuttigh, B., Kramer, M., 2003. Oblique wave transmission over low-crested structures. In: ASCE, Proc. Coastal Structures. 567—579.

Wang, B., Otta, A.K., Chadwick, A.J., 2007. Transmission of obliquely incident waves at low-crested breakwaters: theoretical interpretations of experimental observations. Coastal Eng. 54 (4), 333—344.

Zijlema, M., Stelling, G.S., 2005. Further experiences with computing non-hydrostatic free-surface flows involving water waves. Int. J. Numer. Method Fluids 48 (2), 169—197.

Zijlema, M., Stelling, G., Smit, P., 2011. SWASH: an operational public domain code for simulating wave fields and rapidly varied flows in coastal waters. Coastal Eng. 58 (10), 992—1012.

Zou, Q., Peng, Z., 2011. Evolution of wave shape over a low-crested structure. Coastal Eng. 58 (6), 478—488.